Chemistry of Pentacoordinate [LCuII–Cl]+ Complexes with Quinolyl Containing Tripodal Tetradentate Ligands L

Ning Wei, Narasimha N. Murthy, and Kenneth D. Karlin*

Department of Chemistry, The Johns Hopkins University, Charles & 34th Streets,
Baltimore, Maryland 21218

Ligand design and construction is an important aspect of controlling structure and reactivity in coordination chemistry, and here we describe the synthesis and effects conferred upon the structure, spectroscopy and electrochemistry of [LCuIICl]+ (**1**–**4**), where L is a tripodal tetradentate donor, TMPA (=tris[((2-pyridyl)methyl)-methyl]amine), or corresponding ligands with one (BPQA), two (BQPA), or three (TMQA) 2-quinolyl groups substituted for 2-pyridyl donors. Previous investigations (Karlin, K.; et al. *J. Am. Chem. Soc.* **1993**, *115*, 9506, Wei, N.; et al. *Inorg. Chem.* **1994**, *33*, 1953) have indicated dramatic influences upon stoichiometry, structure and kinetic/thermodynamics in the O$_2$-reactivity with corresponding reduced copper(I) species [LCu(I)]+. Reactions of the quinolyl-containing ligands with copper(II) chloride, followed by metathesis with NaPF$_6$ afforded hexafluorophosphate salts of **2**–**4**. New X-ray structures are reported: [(BPQA)CuCl]·PF$_6$·0.5Et$_2$O (**2-PF$_6$·0.5Et$_2$O**), monoclinic *C2/c*, *a* = 15.509 (3), *b* = 22.945 (4), *c* = 14.745 (5) Å, β = 110.14 (2)°, *Z* = 8, R = 0.049; [(TMQA)CuCl]PF$_6$·CH$_3$CN·0.5Et$_2$O, **4-PF$_6$·CH$_3$CN·0.5Et$_2$O**, monoclinic *C2/c*, *a* = 30.787 (7), *b* = 13.454(8), *c* = 19.927 (9) Å, β = 128.49 (1)°, *Z* = 8, R = 0.054. The coordination geometries about the Cu(II) ion in **2** and **4** are best described as distorted square-based pyramidal, with the latter being nearly perfectly so; the Cl⁻ donor is one of the equitorial ligands. These findings contrast with that observed for [(TMPA)CuIICl]+ (**1**), which is a near-perfect trigonal pyramid, and steric effects of the quinolyl donors appear to be responsible for the distortions in **2**–**4**. The solution structures of **2**–**4** were probed using UV–vis and EPR spectroscopies, suggesting that the solid-state structures observed are maintained in solution, e.g., **2**–**4** manifest typical tetragonal EPR spectra, while that for **1** is "reversed" with $g_\perp$ > $g_\parallel$. Cyclic voltammetric measurements carried out on **1**–**4** in dimethylformamide reveal dramatic effects of the quinolyl for pyridyl replacement in the ligands along the series of complexes. Steric, environmental and/or electronic influences of the quinolyl groups cause an overall increase of ∼0.45 V for $E_{1/2}$ on going from **1** to **4**. Discussions include comparisons of properties with other Cu(I) or Cu(II) complexes with tripodal tetradentate ligands, and the possible relevance to [LCu(I)]+/O$_2$ reaction product structure.

Introduction

We have recently described the reactivity of dioxygen (O$_2$) with copper(I) complexes [LCu(I)]+, where L is a pyridyl and/or quinolyl containing tripodal tetradentate ligand, Chart 1.[1,2] Such ligands are able to stabilize reduced copper(I) ion complexes, without the often encountered problem of disproportionation to Cu(0) and Cu(II), allowing the investigation of L–Cu(I) structure and O$_2$-reactivity.[3–6] The latter processes are of general interest in copper mediated oxidative reactions, and in the bioinorganic chemistry of copper.[5,7–9] In copper protein active sites, O$_2$-binding[10,11] and activation[7–9] processes occur, such as in hemocyanin (molluscan and arthropdal O$_2$-carrier),[10–12]

Chart 1

TMPA

[(TMPA)CuCl]+ (1)

BPQA

[(BPQA)CuCl]+ (2)

BQPA

[(BQPA)CuCl]+ (3)

TMQA

[(TMQA)CuCl]+ (4)
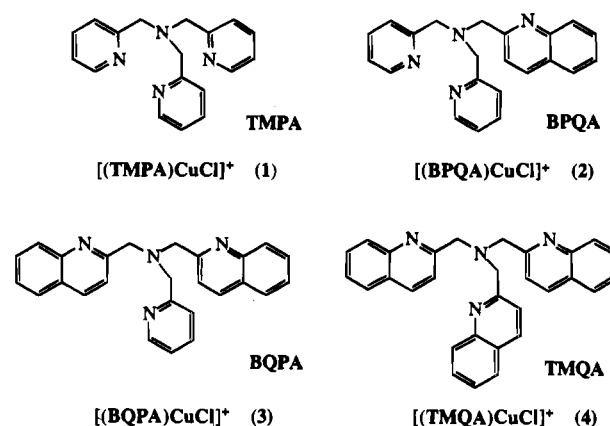
and monooxygenases including tyrosinase,[12] dopamine β-hydroxylase[13,14] and methane monooxygenase.[15] Important O$_2$-binding and reduction reactions also occur in multicopper oxidases (e.g., laccase and ascorbate oxidase),[12,16] in addition to the heme-iron and copper containing cytochrome *c* oxidases.[17–20]

The use of synthetically derived ligands L allows for strong binding to copper ion, and the ability to test how systematically

⊗ Abstract published in *Advance ACS Abstracts,* November 1, 1994.
(1) Karlin, K. D.; Wei, N.; Jung, B.; Kaderli, S.; Pascal, N.; Zuberbühler, A. D. *J. Am. Chem. Soc.* **1993**, 9506–9514.
(2) Wei, N.; Murthy, N. N.; Chen, Q.; Zubieta, J.; Karlin, K. D. *Inorg. Chem.* **1994**, *33*, 1953–1965.
(3) Sorrell, T. N.; Jameson, D. L. *Inorg. Chem.* **1982**, *21*, 1014–1019.
(4) Sorrell, T. N.; Borovik, A. S.; Shen, C.-C. *Inorg. Chem.* **1986**, *25*, 590–591.
(5) Sorrell, T. N. *Tetrahedron* **1989**, *45*, 3–68.
(6) Uozumi, K.; Hayashi, Y.; Suzuki, M.; Uehara, A. *Chem. Lett.* **1993**, *6*, 963–966.
(7) Zuberbühler, A. D. In *Copper Coordination Chemistry: Biochemical and Inorganic Perspectives*; Karlin, K. D., Zubieta, J., Ed.; Adenien: Guilderland, NY, 1983; pp 237–258.
(8) Kitajima, N. *Adv. Inorg. Chem.* **1992**, *39*, 1–77.
(9) *Bioinorganic Chemistry of Copper*; Karlin, K. D.; Tyeklár, Z., Ed.; Chapman & Hall: New York, 1993.

varied steric and/or electronic differences imposed upon the copper complex environment manifest themselves in terms of structure, associated spectroscopy and reactivity patterns. Previously, we studied Cu(I) and Cu(II) complexes with tripodal ligands possessing different donor groups (e.g., pyridyl and thioether)[21,22] or variable chelating ring size,[23–26] and have observed dramatic effects upon the structure, redox potential and spectroscopic features of copper complexes. The study of pyridyl-based tripod ligands containing variable numbers of quinolyl[1,2] (Chart 1) and imidazolyl[27] donor groups is more recent. The effects on copper(I)/O$_2$ reactivity are dramatic and ascribed to a combination of steric and electronic effects.[1,2] [(TMPA)Cu^I(CH$_3$CN)]$^+$ and [(BPQA)Cu^I]$^+$ react with O$_2$ leading to thermodynamically stable Cu/O$_2$ = 2:1 peroxo dicopper(II) complexes [{LCu}$_2$(O$_2$)]$^{2+}$, with a *trans-μ*-1,2 peroxodicopper(II) coordination.[2,26,28] By contrast, [(BQPA)-Cu^I] forms a more stable Cu/O$_2$ = 1:1 adduct [{(BQPA)Cu}-(O$_2$)]$^+$ (described as a superoxo—copper(II) species, but with detailed structure unknown), and [(TMQA)Cu^I] is completely unreactive toward dioxygen.[1,2] The complete kinetics and thermodynamics of formation of these copper-dioxygen adducts have been detailed.[1,2]

Like all metal—dioxygen reactions,[29] Cu(I)/O$_2$ reactions involve some degree of electron-transfer. Thus, the structures and physical properties of copper(II) analogues of LCu^I species are of interest, since the ligation and coordination geometry observed in such Cu(II) species may closely resemble that seen in Cu$_n$O$_2$ (n = 1 or 2) adducts, and the latter structure may be unknown. In this report, we describe the synthesis and characterization of chloride complexes [LCu^{II}Cl]$^+$ (1—4, Chart 1), and the differences in properties observed as a consequence of variations in L. While Cl$^-$ does not directly serve as a superoxo or peroxo surrogate, it forms stable easily characterizable complexes with Cu(II), providing an additional ligand

(10) Volbeda, A.; Hol, W. G. J. *J. Mol. Biol.* **1989**, *209*, 249–279.
(11) Hazes, B.; Magnus, K. A.; Bonaventura, C.; Bonaventura, J.; Dauter, Z.; Kalk, K.; Hol, W. G. J. *Protein Sci.* **1993**, *2*, 597–619.
(12) Solomon, E. I.; Baldwin, M. J.; Lowery, M. D. *Chem. Rev.* **1992**, *92*, 521–542.
(13) Tian, G.; Berry, J. A.; Klinman, J. P. *J. Am. Chem. Soc.* **1994**, *33*, 226–234.
(14) Reedy, B. J.; Blackburn, N. J. *J. Am. Chem. Soc.* **1994**, *116*, 1924–1931.
(15) Nguyen, H.-H. T.; Shiemke, A. K.; Jacobs, S. J.; Hales, B.; Lidstrom, M. E.; Chan, S. I. *J. Biol. Chem.* **1994**, *269*, 14995–15005.
(16) Messerschmidt, A. In *Bioinorganic Chemistry of Copper*; Karlin, K. D., Tyeklár, Ed.; Chapman & Hall: New York, 1993; pp 471–484.
(17) Malmström, B. G. *Acc. Chem. Res.* **1993**, *26*, 332–338.
(18) Fee, J. A.; Antholine, W. E.; Fan, C.; Gurbiel, R. J.; Surerus, K.; Werst, M.; Hoffman, B. M. In *Bioinorganic Chemistry of Copper*; Karlin, K. D., Tyeklár, Z., Ed.; Chapman & Hall: New York, 1993; pp 485–500.
(19) Babcock, G. T.; Wilkström, M. *Nature* **1992**, *356*, 301–309.
(20) A mini review series devoted to cytochrome *c* oxidase appears in the following: *J. Bioenerg. Biomembr.* **1993**, *25* (2), 69–188.
(21) Karlin, K. D.; Dahlstrom, P. L.; Hyde, J. R.; Zubieta, J. *J. Chem. Soc. Chem. Commun.* **1980**, *906*, 906–908.
(22) Karlin, K. D.; Yandell, J. K. *Inorg. Chem.* **1984**, *23*, 1184–1188.
(23) Karlin, K. D.; Hayes, J. C.; Juen, S.; Hutchinson, J. P.; Zubieta, J. *Inorg. Chem.* **1982**, *21*, 4106–4108.
(24) Zubieta, J.; Karlin, K. D.; Hayes, J. C. In *Copper Coordination Chemistry: Biochemical and Inorganic Perspectives*; Karlin, K. D., Zubieta, J., Ed.; Adenine Press: Albany, N.Y., 1983; pp 97–108.
(25) Jacobson, R. R. Ph.D. Dissertation Thesis, State University of New York (SUNY) at Albany, 1989.
(26) Tyeklár, Z.; Jacobson, R. R.; Wei, N.; Murthy, N. N.; Zubieta, J.; Karlin, K. D. *J. Am. Chem. Soc.* **1993**, *115*, 2677–2689.
(27) Wei, N.; Murthy, N. N.; Tyeklár, Z.; Karlin, K. D. *Inorg. Chem.* **1994**, *33*, 1177–1183.
(28) Jacobson, R. R.; Tyeklár, Z.; Karlin, K. D.; Liu, S.; Zubieta, J. *J. Am. Chem. Soc.* **1988**, *110*, 3690–3692.
(29) Gubelmann, M. H.; Williams, A. F. *Struct. Bonding (Berlin)* **1983**, *55*, 1–65.

Table 1. Crystallographic Data for [(BPQA)CuCl]PF$_6$·^{1}/$_2$Et$_2$O (**2-PF$_6$**(^{1}/$_2$Et$_2$O) and [(TMQA)CuCl]PF$_6$·CH$_3$CN·^{1}/$_2$Et$_2$O (**4-PF$_6$**·CH$_3$CN·^{1}/$_2$Et$_2$O)

	2-PF$_6$·^{1}/$_2$Et$_2$O	4-PF$_6$·CH$_3$CN·^{1}/$_2$Et$_2$O
formula	C$_{24}$H$_{20}$CuClN$_4$O$_{0.5}$PF$_6$	C$_{34}$H$_{24}$ClN$_5$O$_{0.5}$PF$_6$Cu
temp, nK	153	163
MW	621.45	754.56
cryst system	monoclinic	monoclinic
space group	C2/c	C2/c
a, Å	15.509(3)	30.787(7)
b, Å	22.945(4)	13.454(8)
c, Å	14.745(5)	19.927(9)
α, deg	90.00	90.00
β, deg	110.14(2)	128.49(1)
γ, deg	90.00	90.00
V, Å^3	4926(2)	6461(5)
F(000)	2528	3056
Z	8	8
D$_{calcd}$, g/cm^3	1.676	1.551
abs coeff, cm^{-1}	11.30	8.77
no. of unique refcns collcd	4486	5938
no. of indept reflcns	2785 ($\leq 3\sigma$(I))	3395 ($\geq 3\sigma$(I))
no. of refined params (Nv)	336	401
largest peak/hole, e Å^{-3}	0.93/−0.80	0.77/−0.58
R^a	0.049	0.054
R$_w$^{b}	0.052	0.051

^{a} $R = \Sigma[|F_o| - |F_c|/\Sigma|F_o|]$. ^{b} $R_w = [\Sigma w(|F_o| - |F_c|)^2/\Sigma w|F_o|^2]^{1/2}$.

compared to the Cu(I)—ligand complex; the coordination number usually increases when Cu(I) complexes are converted to Cu(II)-analogues. The X-ray structures of [(BPQA)CuCl]$^+$ (**2**) and [(TMQA)CuCl]$^+$ (**4**) are described, while comparisons and contrasts in UV—vis and EPR spectroscopic properties, and Cu(II)/Cu(I) redox potentials are provided.

Synthesis and X-ray Structures of Copper(II) Complexes. [(TMPA)CuCl]PF$_6$ (**1-PF$_6$**) was previously synthesized and structurally characterized.[23,25] It possesses a trigonal bipyramidal geometry with Cl$^-$ and tertiary alkylamino N-atoms axially coordinated; the three pyridyl nitrogens in TMPA occupy equatorial sites. Pentacoordinate Cu(II) complexes [LCuCl]PF$_6$ (**2—4**) were synthesized (Experimental Section) by reacting equivalent amounts of CuCl$_2$·2H$_2$O and the appropriate tripodal ligand in methanol solvent. Excess NaPF$_6$ were added to exchange the Cl$^-$ anion, also causing precipitation of desired copper complex products. Purification to remove NaCl and excess NaPF$_6$ was accomplished by recrystallization from CH$_2$Cl$_2$/Et$_2$O.

Structure of [(BPQA)CuCl]PF$_6$·^{1}/$_2$Et$_2$O (2-PF$_6$·^{1}/$_2$Et$_2$O). X-ray quality crystals (**2-PF$_6$**)·^{1}/$_2$Et$_2$O were obtained by recrystallizing the complex from CH$_3$CN/Et$_2$O. A summary of the crystal and refinement data is given in Table 1, while atomic coordinates and isotropic thermal parameters are found in Table 2. Selected bond lengths and angles are provided in Table 3 and an ORTEP diagram of the cationic portion of the complex is shown in Figure 1.

The structure of the [(BPQA)CuCl]$^+$ (**2**) cation reveals the copper(II) ligated to two pyridyl, one quinolyl and one tertiary alkylamino nitrogen atoms. The pentacoordination is completed by the chloride ligand. The geometry about the Cu(II) ion was analyzed by a convenient method described by Addison and Reedijk,[30] in which a parameter τ, calculated using observed L—M—L' basal angles, is an index of the degree of trigonality of the structure. Within the structural continuum between trigonal bipyramidal and square pyramidal limiting geometries, τ is equal to zero for a perfect square pyramidal or tetragonal geometry; it becomes unity for a perfect trigonal bipyramidal

(30) Addison, A. W.; Rao, T. N.; Reedjik, J.; Rijn, J. V.; Verschoor, G. C. *J. Chem. Soc., Dalton Trans.* **1984**, 1349–1356.

Table 2. Positional Parameters and B(eq) for [Cu(BPQA)Cl](PF$_6$)·0.5Et$_2$O (2-PF$_6$·0.5Et$_2$O) and [Cu(TMQA)Cl](PF$_6$)·CH$_3$CN·0.5$_2$O (4-PF$_6$·CH$_3$CN·0.5Et$_2$O)

atom	x	y	z	B (eq)	atom	x	y	z	B (eq)
				2-PF$_6$·0.5Et$_2$O					
Cu(1)	0.79352(5)	0.17446(3)	0.06666(6)	2.42(3)	C(32)	0.8717(5)	0.2636(3)	0.3383(6)	4.0(3)
Cl(1)	0.8800(1)	0.24292(7)	0.0288(1)	3.76(7)	C(33)	0.7995(5)	0.2502(3)	0.3690(5)	3.9(3)
P(1)	0.3860(1)	0.09554(7)	0.0540(1)	2.65(7)	C(34)	0.7300(4)	0.2141(3)	0.3121(5)	3.0(3)
F(1)	0.4811(2)	0.0624(2)	0.1041(3)	4.0(2)	C(35)	0.7337(4)	0.1946(2)	0.2256(5)	2.4(2)
F(2)	0.2910(2)	0.1288(2)	0.0039(3)	4.5(2)	C(36)	0.6584(4)	0.1581(3)	0.1556(4)	2.4(2)
F(3)	0.4146(3)	0.1088(2)	−0.0366(3)	6.5(3)	C(36)	0.6584(4)	0.1581(3)	0.1556(4)	2.4(2)
F(4)	0.3568(2)	0.0832(2)	0.1449(3)	5.4(2)	C(41)	0.9656(4)	0.0728(2)	0.1103(4)	1.8(2)
F(5)	0.3404(3)	0.0364(2)	0.0075(3)	5.7(2)	C(42)	1.0240(4)	0.1149(3)	0.0905(4)	2.5(2)
F(6)	0.4322(3)	0.1548(2)	0.1016(4)	6.5(2)	C(43)	1.1066(4)	0.0985(3)	0.0840(4)	2.7(3)
N(1)	0.6986(3)	0.1219(2)	0.0963(3)	1.9(2)	C(44)	1.1355(4)	0.0396(3)	0.0982(4)	2.7(3)
N(2)	0.7420(3)	0.1385(2)	−0.0645(4)	2.6(2)	C(45)	1.0808(4)	−0.0014(3)	0.1169(4)	2.6(3)
N(3)	0.8026(3)	0.2083(2)	0.1934(4)	2.5(2)	C(46)	0.9941(4)	0.0139(3)	0.1226(4)	2.1(2)
N(4)	0.8833(3)	0.0905(2)	0.1179(3)	1.9(2)	C(47)	0.9326(4)	−0.0275(2)	0.1374(4)	2.3(2)
C(21)	0.7753(5)	0.1431(3)	−0.1374(4)	3.4(3)	C(48)	0.8518(4)	−0.0099(2)	0.1430(4)	2.0(2)
C(22)	0.7362(6)	0.1142(3)	−0.2230(6)	4.5(4)	C(49)	0.8297(4)	0.0505(2)	0.1344(4)	1.9(2)
C(23)	0.6629(6)	0.0778(3)	−0.2355(5)	4.4(4)	C(50)	0.7455(4)	0.0709(2)	0.1538(4)	2.2(2)
C(24)	0.6290(5)	0.0718(3)	−0.1607(5)	3.6(3)	C(2)	0.9210(5)	0.1899(2)	0.6337(6)	3.0(3)
C(25)	0.6689(4)	0.1036(3)	−0.0772(5)	2.7(3)	C(1)	0.9858(6)	0.1990(3)	0.6576(6)	3.8(3)
C(26)	0.6294(4)	0.1042(3)	0.0034(4)	2.5(2)	O(1)	1.0000	0.219(1)	3/4	23.1(8)
C(31)	0.8714(4)	0.2426(3)	0.2514(5)	3.4(3)					
				4-PF$_6$·CH$_3$CN·0.5Et$_2$O					
Cu(1)	0.68121(3)	0.09861(6)	0.71632(5)	1.65(3)	C(33)	0.5163(3)	0.0053(5)	0.6663(5)	2.9(3)
Cl(1)	0.68144(7)	−0.0565(1)	0.6751(1)	2.70(7)	C(34)	0.4623(3)	0.0341(6)	0.5933(5)	3.5(3)
N(1)	0.6903(2)	0.2205(4)	0.6567(3)	2.0(2)	C(35)	0.4547(3)	0.0883(6)	0.5293(5)	3.2(3)
N(2)	0.7655(2)	0.1053(4)	0.7959(3)	1.6(2)	C(36)	0.5002(3)	0.1184(5)	0.5344(4)	2.5(3)
N(3)	0.6002(2)	0.1229(4)	0.6157(3)	1.7(2)	C(37)	0.4942(3)	0.1722(6)	0.4684(4)	2.9(3)
N(4)	0.6801(2)	0.2123(4)	0.7877(3)	1.6(2)	C(38)	0.5406(3)	0.2004(5)	0.4774(4)	2.7(3)
P(1)	0.63293(8)	0.2039(1)	0.3501(1)	2.53(8)	C(39)	0.5930(3)	0.1752(5)	0.5526(4)	2.2(3)
F(1)	0.5956(2)	0.2610(3)	0.3676(3)	4.2(2)	C(40)	0.6447(3)	0.2032(5)	0.5651(4)	2.3(3)
F(2)	0.6819(2)	0.1949(4)	0.4515(3)	4.4(2)	C(41)	0.6782(3)	0.2050(5)	0.8546(4)	1.8(3)
F(3)	0.6587(2)	0.3074(3)	0.3497(3)	3.9(2)	C(42)	0.6748(3)	0.1109(5)	0.8818(4)	2.0(3)
F(4)	0.6706(2)	0.1457(3)	0.3329(3)	4.1(2)	C(43)	0.6740(3)	0.1024(6)	0.9494(4)	2.5(3)
F(5)	0.5849(2)	0.2137(3)	0.2485(2)	3.6(2)	C(44)	0.6756(3)	0.1876(6)	0.9922(5)	3.1(3)
F(6)	0.6079(2)	0.1005(3)	0.3508(3)	3.9(2)	C(45)	0.6786(3)	0.2789(6)	0.9667(5)	3.1(3)
C(21)	0.8010(3)	0.0570(5)	0.8729(4)	1.7(2)	C(46)	0.6797(3)	0.2901(5)	0.8979(4)	2.4(3)
C(22)	0.7793(3)	−0.0122(5)	0.8986(4)	2.0(3)	C(47)	0.6840(3)	0.3833(5)	0.8705(5)	3.2(3)
C(23)	0.8144(3)	−0.0586(5)	0.9769(4)	2.3(3)	C(48)	0.6854(3)	0.3893(5)	0.8037(5)	2.8(3)
C(24)	0.8714(3)	−0.0391(5)	1.0308(5)	3.1(3)	C(49)	0.6827(3)	0.3023(5)	0.7627(4)	2.0(3)
C(25)	0.8931(3)	0.0266(6)	1.0056(5)	3.1(3)	C(50)	0.6831(3)	0.3136(5)	0.6880(4)	2.2(3)
C(26)	0.8586(3)	0.0745(5)	0.9260(4)	2.1(3)	C(1)	0.0489(7)	0.013(1)	0.148(1)	14.8(6)
C(27)	0.8787(3)	0.1418(5)	0.8973(5)	2.8(3)	N(5)	0.0463(6)	0.088(1)	0.099(1)	17.0(5)
C(28)	0.8436(3)	0.1870(5)	0.8201(5)	2.8(3)	C(2)	0.0435(7)	−0.061(1)	0.193(1)	14.8(6)
C(29)	0.7864(3)	0.1656(5)	0.7701(4)	1.9(3)	O(1)	1.0000	0.253(2)	1/4	25.7
C(30)	0.7462(3)	0.2109(5)	0.6814(4)	2.5(3)	C(3)	1.0069	0.1390	0.2269	31.8
C(31)	0.5545(2)	0.0932(5)	0.6079(4)	2.0(2)	C(4)	1.0316	0.0729	0.2228	59.7
C(32)	0.5609(3)	0.0343(5)	0.6716(4)	2.4(3)					

Table 3. Selected Bond Distances (Å) and Angles (deg) for Cu(II) Complexes

2-PF$_6$·^{1}/$_2$Et$_2$O		4-PF$_6$·CH$_3$CN·^{1}/$_2$Et$_2$O		1-PF$_6$	
			Bond Distances		
Cu−Cl(1)	2.257(2)	Cu−Cl(1)	2.244(2)	Cu−Cl(1)	2.233(2)
Cu−N(1)	2.063(4)	Cu−N(1)	2.144(5)	Cu−N(1)	2.050(6)
Cu−N(2)	1.999(5)	Cu−N(2)	2.033(5)	Cu−N(2)	2.062(8)
Cu−N(3)	1.998(6)	Cu−N(3)	2.030(5)	Cu−N(3)	2.060(9)
Cu−N(4)	2.345(4)	Cu−N(4)	2.104(5)	Cu−N(4)	2.072(6)
			Bond Angles		
Cl(1)−Cu−N(1)	170.9(1)	Cl(1)−Cu−N(1)	118.5(2)	Cl(1)−Cu−N(1)	179.1(4)
Cl(1)−Cu−N(2)	97.0(2)	Cl(1)−Cu−N(2)	91.9(2)	Cl(1)−Cu−N(2)	97.6(3)
Cl(1)−Cu−N(3)	96.0(2)	Cl(1)−Cu−N(3)	94.0(2)	Cl(1)−Cu−N(3)	99.6(3)
Cl(1)−Cu−N(4)	108.3(1)	Cl(1)−Cu−N(4)	158.2(2)	Cl(1)−Cu−N(4)	99.4(2)
N(1)−Cu−N(2)	83.5(2)	N(1)−Cu−N(2)	81.7(2)	N(1)−Cu−N(2)	81.5(4)
N(1)−Cu−N(3)	81.6(2)	N(1)−Cu−N(3)	80.4(2)	N(1)−Cu−N(3)	81.1(4)
N(1)−Cu−N(4)	80.8(2)	N(1)−Cu−N(4)	83.2(2)	N(1)−Cu−N(4)	80.8(3)
N(2)−Cu−N(3)	161.5(2)	N(2)−Cu−N(3)	161.8(2)	N(2)−Cu−N(3)	118.2(3)
N(2)−Cu−N(4)	88.1(2)	N(2)−Cu−N(4)	89.5(2)	N(2)−Cu−N(4)	118.8(3)
N(3)−Cu−N(4)	100.1(2)	N(3)−Cu−N(4)	91.4(2)	N(3)−Cu−N(4)	116.0(3)

arrangement. Based on this calculation, $\tau = 0.16$ for [(BPQA)-CuCl]$^+$, indicating that the structure can be best described as a slightly distorted square-based pyramid. Atoms N(1), N(2), N(3), and Cl(1) (Figure 1) form the best basal plane; the Cu

atom deviates by 0.183 Å from this plane in the direction of the axial quinolyl N4 atom. The latter forms relatively longer bonds with the Cu(II) ion (Cu(1)−N(4) = 2.341 Å), compared to the other three Cu−nitrogen bonds (Table 3). The Cu−
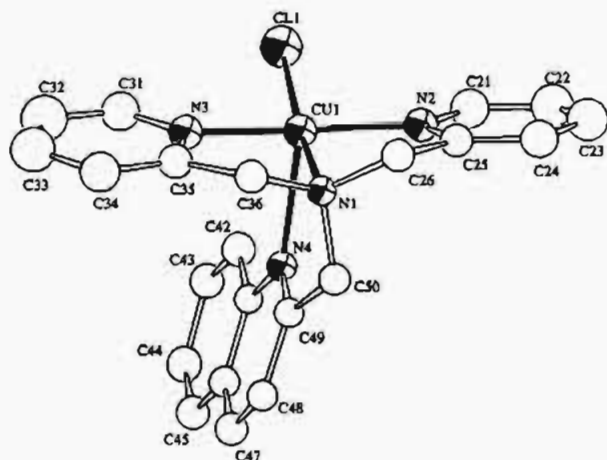
Figure 1. ORTEP diagram (50% elipsoids) of the cationic portion of [(BPQA)CuCl]$^+$ (2) showing the atom labeling scheme.

$N_{pyridyl}$ bonds of **2** (2.00 Å, Table 3) in the equatorial plane are slightly shorter than those observed in [(TMPA)CuCl]$^+$ (see diagram below with PY = 2-pyridyl; Cu–N$_{pyridyl}$ = 2.06–2.07 Å, Table 3),[23] where a nearly perfect trigonal bipyramidal structure is observed; there, the pyridyl nitrogens comprise the equatorial plane and $\tau = 1.01$.[31]
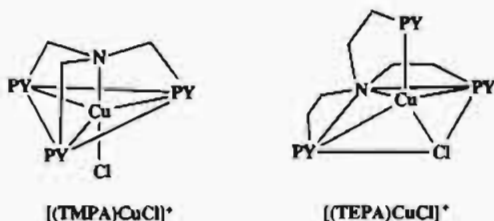
[(TMPA)CuCl]$^+$ [(TEPA)CuCl]$^+$

The structure of [(BPQA)CuCl]$^+$ (**2**) is closer to that found for [(TEPA)CuCl]$^+$,[23] (TEPA = tris(2-pyridylethyl)amine), with its three six- (rather than five-) membered chelate rings; this complex adopts a nearly square-based pyramidal coordination geometry, $\tau = 0.19$.

Thus, even the replacement of a single pyridyl group in the tetradentate TMPA ligand by one quinolyl donor causes a substantive geometric change in the pentacoordinate environment, where Cl$^-$ is an exogenous anionic ligand. These geometries are roughly maintained in solution, as indicated by the spectroscopic studies described below. The results further illustrate how particular synthetically derived ligands exercise considerable environmental influences and dictate copper(II) ion geometries.

Structure of [(TMQA)CuCl]PF$_6$·CH$_3$CN·^{1}/$_2$Et$_2$O (4-PF$_6$·CH$_3$CN·^{1}/$_2$Et$_2$O). X-ray quality crystals **4-PF$_6$·CH$_3$CN·^{1}/$_2$Et$_2$O** were also obtained by recrystallizing the complex from CH$_3$CN/Et$_2$O. Crystal data, refinement parameters, and coordinates with thermal parameters are given in Tables 1 and 2, respectively, while selected bond distances and angles are listed in Table 3. An ORTEP diagram of the cation **4** is shown in Figure 2.

The copper(II) ion in [(TMQA)CuCl]$^+$ (**4**) is coordinated to three quinolyl nitrogen atoms, a chloride ion, and the "hard"
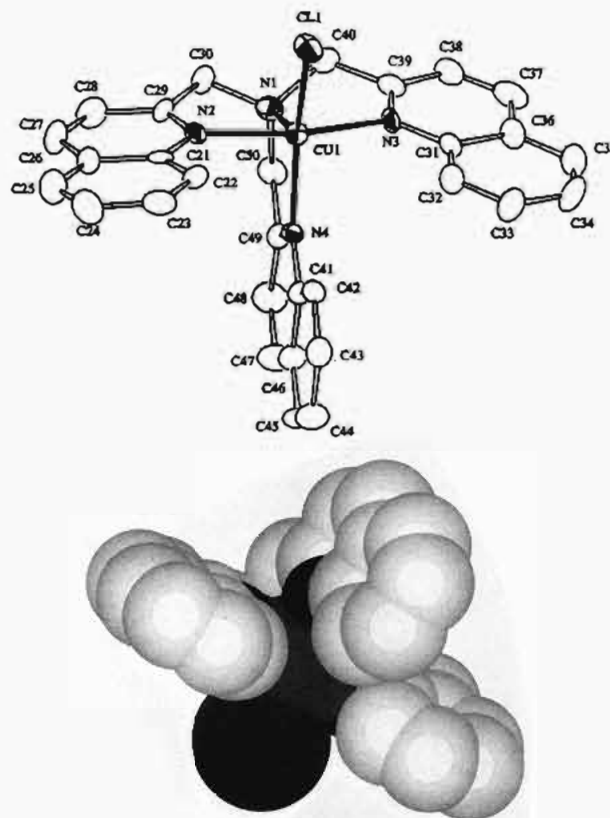
Figure 2. (a) ORTEP diagram (50% elipsoids) of the cationic portion of [(TMQA)CuCl]$^+$ (**4**) showing the atom labeling scheme. (b) Space filling diagram of Chem 3D drawing of [(TMQA)CuCl]$^+$ (**4**) rotated ~180°.

tertiary amine nitrogen. In this structure $\tau = 0.06$, i.e., the complex is only slightly distorted from perfect square pyramidal coordination. Quinolyl nitrogen atoms N(2), N(3), N(4), plus Cl comprise the best basal plane and the Cu(II) ion lies 0.13 Å out of this, toward the N(1) atom. Thus, Cu–N(1) is the axial bond at a distance of 2.14 Å. The Cu–N$_{quinolyl}$ distances range from 2.03 to 2.10 Å and are longer than those found in tetracoordinated Cu(I) complex (2.00–2.02 Å) with the same ligand.[2] The lengthening of Cu(II)–N$_{quinolyl}$ bonds in this complex compared to its Cu(I) analogue may be explained by the increased coordination number around the Cu(II) center in **4**. However, these Cu–N$_{quinolyl}$ distances are comparable to those observed for the pentacoordinate [(TEPA)CuCl]$^+$ complex (Cu–N$_{pyridyl}$ = 2.04–2.06)[23] which has essentially the same coordination geometry (vide supra).

The observed structure of [(TMQA)CuCl]$^+$ (**4**) further supports the finding that substitution of quinolyl for pyridyl groups in the series of ligands going from TMPA to TMQA (Chart 1) leads to changes in the coordination geometries of derived copper(II) complexes. An examination and judgment of steric interactions reveals the likely origin of these findings. Complexes with TMPA, e.g., [(TMPA)Cu–X]$^{n+}$ (X = Cl$^-$ (**1**), F$^-$,[32] CH$_3$CN[25], O$_2$$^{2-}$[26]) possess a trigonal bipyramidal geometry. Inspection of hand-held molecular or space-filling computer models readily show why such a geometry is not maintained for [(TMQA)Cu–X]$^{n+}$; the fifth X ligand would fall deep into the pocket formed by the three quinolyl donors, and there would be severe overlap between X (especially for a large X = Cl$^-$ ligand) and the quinolyl 8-hydrogens (see space-

---

(31) The value greater than one indicates the Cu in not exactly in the equatorial plane, but slightly above, toward the apical alkylamino nitrogen atom.

(32) Jacobson, R. R.; Tyeklár, Z.; Karlin, K. D.; Zubieta, J. *Inorg. Chem.* **1991**, *30*, 2036–2040.

Table 4. Electronic Spectra Data (cm^{-1}) (CH$_3$CN) and EPR Parameters (DMF) of Cu(II) Complexes

complexes	d—d	CT	EPR params			
			$g_{\parallel}$	$g_{\perp}$	$A_{\parallel}$ (cm^{-1})	$A_{\perp}$ (cm^{-1})
[TMPA)CuCl]$^{+ 23}$ (**1**)	725 (sh, 90)	247 (3220)	2.01^{40}	2.18^b		96
	955 (210)	256 (12500)				
[(BPQA)CuCl]$^+$ (**2**)	700 (sh, 106)	300 (5800)	2.20	2.03	128	
	897 (150)	316 (4650)				
[(BQPA)CuCl]$^+$ (**3**)	737 (137)	300 (15000)_	2.24	2.07	136	
	862 (139)	316 (12400)				
[(TMQA)CuCl]$^+$ (**4**)	691 (185)	303 (12200)	2.24	2.06	139	
	1000 (sh, 90)	316 (15800)				
[(TEPA)CuCl]$^{+ 23}$	669 (199)	259 (14100)	2.23		159	
	971 (sh, 47)	285 (sh 4320)				

filling picture):

Such interactions would not exist in comparable Cu(II) complexes with the pyridyl-containing TMPA ligand, as manifested by the existence of [(TMPA)Cu—X]$^{n+}$ (vide supra). Thus, in [(TMQA)Cu—X]$^{n+}$ (e.g., **4**) and other quinolyl containing complexes such as **2** and **3**, a twisting or distortion occurs, giving rise to tetragonally coordinated species.

Note that in **4** (Figure 2), the chloride ligand is in an equatorial position of the square-based pyramid and interactions with the quinolyl groups are minimized by having the Cu—Cl(1) vector nearly perpendicular to the Cu—N(2) and Cu—N(3) bonds (Figure 2). Also, the Cu—Cl(1) vector is nearly perpendicular to the quinolyl rings containing N(2) and N(3); these lie essentially perpendicular to the complex basal plane and are nearly coplanar themselves. It is interesting to note that we do not observe a structure in which the Cl$^-$ ligand lies in the N(1),N(2),N(3) plane opposite to N(1) (with the quinolyl N(4) axial); this would also be disfavored because of Cl$^-$-with-quinolyl (8-H) steric interactions (see Figure 2b). Thus, the quinolyl ligands exercise pronounced structural effects upon the complexes when replacing pyridyl donors, due to their bulkiness and resulting steric interactions.

Electronic and EPR Spectroscopy of [LCu^{II}Cl]$^+$ (1—4). UV—vis and electron paramagnetic resonance spectroscopic properties (Table 4) of **1—4** also vary systematically along the series of quinolyl containing complexes, supporting the conclusion that basic elements of the solid-state structures are maintained in solution.

All four chloride—Cu(II) complexes possess intense high-energy absorptions in the 300—315 nm region, typically found for pyridyl containing cupric complexes,[33] assigned to ligand-to-metal charge transfer transitions. Weaker d—d absorptions in the 650—1000 nm region are observed, and the pattern of bands and their relative intensities are often diagnostic of the
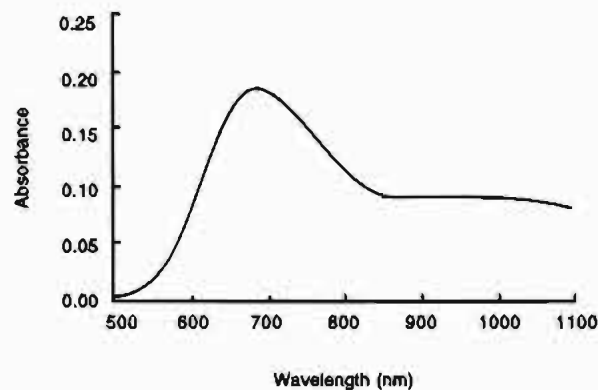
Figure 3. Room temperature UV—vis spectrum of [(TMQA)CuCl]$^+$ in CH$_3$CN.

exact nature of the pentacoordinate geometry. Thus, the presence of one peak accompanied by a higher energy (less-intense) shoulder is typical of a trigonal bipyramidal Cu(II) coordination.[23-25,33-38] On the other hand, when a Cu(II) ion has a square-pyramidal coordination, the reverse absorption pattern is normally observed, i.e., a high energy peak with a low energy shoulder.[23-25,33-38] Precisely these trends are observed for [(TMPA)CuCl]$^+$ (**1**) and [(TEPA)CuCl]$^+$ (vide supra), where the solution structure have also been corroborated by EPR spectroscopy.[23]

For [(TMQA)CuCl]$^+$ (**4**), the UV—vis spectrum in acetonitrile (Figure 3 and Table 4) is distinctively different than that observed for a trigonal bipyramidal complex such as [(TMPA)-CuCl]$^+$ (**1**), and both UV—vis and EPR (vide infra) data are consistent with a square-based pyramidal structure, like that of [(TEPA)CuCl]$^+$. This is consistent with the observed solid-state structure, described above.

On the other hand, [(BPQA)CuCl]$^+$ (**2**), exhibits two absorptions with only a slightly higher intensity for the low energy band (Table 4), suggesting an intermediate structure, or perhaps one closer to trigonal bipyramidal. [(BQPA)CuCl]$^+$ (**3**) possesses two bands of nearly equal intensity (Table 4), also suggestive of a distorted solution structure. We therefore conclude that when the ligand environment changes from TMPA to TMQA, with quinolyl for pyridyl substitution, the geometry around Cu(II) gradually changes from a trigonal bipyramidal to square pyramidal coordination.

The EPR data (Table 4) actually indicate that only [(TMPA)-CuCl]$^+$ (**1**) exhibits a trigonal electronic ground state (i.e. d_{z^2}).

(33) Hathaway, B. J. In *Comprehensive Coordination Chemistry*; Wilkinson, G., Ed.; Pergamon: New York, 1987; Vol. 5; pp 533—774.

(34) Thompson, L. K.; Ramaswamy, B. S.; Dawe, R. D. *Can. J. Chem.* **1978**, *56*, 1311.

(35) Duggan, M.; Ray, N.; Hathaway, B.; Tomlinson, G.; Briant, P.; Plein, K. *J. Chem. Soc. Dalton Trans.* **1980**, 1342.

(36) Thompson, L. K.; Ramaswamy, B. S.; Seymout, E. A. *Can. J. Chem.* **1977**, *55*, 878.

(37) Addison, A. W.; Hendricks, H. M.; Reedijk, J.; Thompson, L. K. *Inorg. Chem.* **1981**, *20*, 103—110.

(38) Barbucci, R.; Bencini, A.; Gatteschi, D. *Inorg. Chem.* **1977**, *16*, 2117.
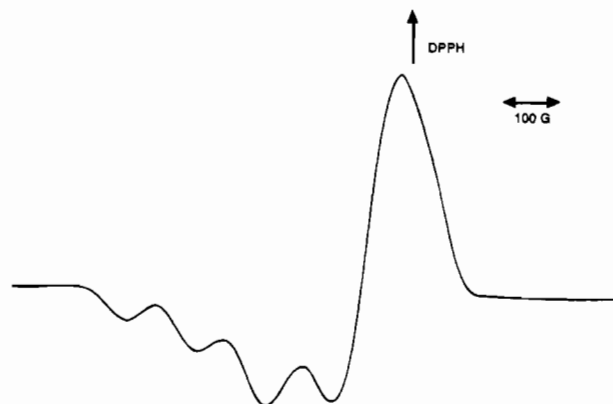
Figure 4. Electron paramagnetic resonance spectrum of [(TMQA)-CuCl]$^+$ in frozen DMF solution.

Table 5. Cyclic Voltammetry Data of Copper Complexes in DMF

complexes	$E_{1/2}(V)^a$	ΔE_p (mV)	i_{pa}/i_{pc}
[(TMPA)CuCl]$^+$ (**1**)	−0.79	91	0.80
[(BPQA)CuCl]$^+$ (**2**)	−0.67	85	0.80
[(BQPA)CuCl]$^+$ (**3**)	−0.52	94	0.80
[(TMQA)CuCl]$^+$ (**4**)	−0.34	94	1.04
[(TMPA)Cu(CH$_3$CN)]$^+$ ^{2}	−0.61	78	0.80
[(BPQA)Cu]$^+$ ^{2}	−0.53	85	0.96
[(BQPA)Cu]$^+$ ^{2}	−0.41	95	0.96
[(TMQA)Cu]$^+$ ^{2}	−0.24	108	1.02

^{a} Ag/AgNO$_3$ reference electrode.

Any distortion caused by the presence of quinolyl donors in complexes [(L)Cu^{II}Cl]$^+$ (**2**–**4**) gives rise to species with a $d_{x^2-y^2}$ ground state, i.e. with characteristic tetragonal (axial) EPR pattern. EPR spectral differences are quite apparent for these two cases, where tetragonally coordinated Cu(II) complexes show features with $g_{||} > 2.1 > g_{\perp} > 2.0$ and $A_{||} = 130-190 \times 10^{-4}$ cm^{-1}.[39] The $g_{||}$ and $A_{||}$ values are strongly affected by the ligand environment in a tetragonal cupric site. Increasing field strength of the equatorial ligands causes $g_{||}$ to decrease and $A_{||}$ to increase, while increased covalency leads to a decrease in both values.

This is exactly what is observed for [(L)Cu^{II}Cl]$^+$ (**2**–**4**) (Table 4), as illustrated in the frozen solution (DMF) EPR spectrum of [(TMQA)CuCl]$^+$ (**4**), Figure 4. The expected hyperfine splitting due to the $I = ^3/_2$ nuclear spin on copper is well resolved in the $g_{||}$ region and the spin-Hamiltonian parameters (Table 4) are typical. EPR spectra and parameters for [(L)Cu^{II}Cl]$^+$ (**2**–**4**) are all very similar, indicating axial ground state electronic structures; any minor distortions from square pyramidal geometry which exist in the complexes [(BPQA)CuCl]$^+$ (**2**) and [(BQPA)CuCl]$^+$ (**3**) are not obvious from an examination of their EPR spectra. The $A_{||}$ values are relatively smaller than found for [(TEPA)CuX]$^+$ (X = Cl$^-$, SCN$^-$ and N$_3^-$; $g_{||} = 2.21$ to 2.25; $A_{||} = (133-176) \times 10^{-4}$ cm^{-1}).[25] Only [(TMPA)-CuCl]$^+$, possessing a trigonal bipyramidal structure in the solid state and solution, shows the expected reversal of parallel and perpendicular regions in its EPR spectrum ($g_{\perp} = 2.18$ and $A_{||} = 96 \times 10^{-4}$ cm^{-1}).[23,25,36–38,40]

Electrochemistry. The half wave potential for all Cu(II) complexes [LCu^{II}Cl]$^+$ (**1**–**4**) were measured by cyclic voltammetry (CV) under argon in dimethylformamide (DMF) solvent and the results are given in Table 5. The CV's are well-behaved and display a single quasi-reversible one electron redox wave with i_{pa}/i_{pc} approaching unity, varying over the range 0.80–
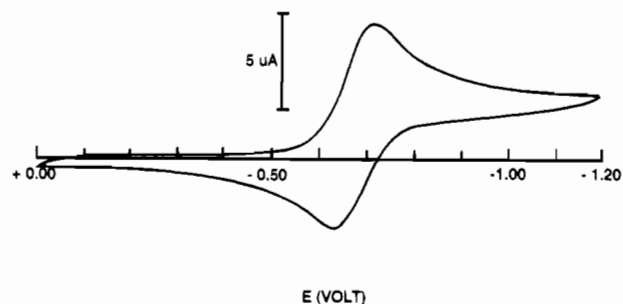
Figure 5. Cyclic voltammetry of [(BPQA)CuCl]$^+$ in DMF.

1.02. Peak separations were less than 110 mV at a scan rate of 100 mV/s. The ferrocene/ferrocenium couple under the same conditions exhibited $\Delta E_p = 89$ mV and $E_{1/2} = 20$ mV vs Ag/AgNO$_3$. A typical CV scan for [(BPQA)CuCl]$^+$ (**2**) is given in Figure 5.

The data reveals that as quinolyl groups replace pyridyl ligand donors in the series of complexes **1**–**4**, the half-wave potential becomes significantly more positive (Table 5). Many factors are known to influence the redox potentials of copper complexes including (a) the flexibility or constraints imposed by chelating ligands, which might favor a geometry preferred by one metal ion oxidation state, but not the other, (b) the types of donor atoms (i.e., O vs N vs S) and (c) the geometry of coordinated complexes.[24,33,41–44] Here, one effect that probably contributes to the variations observed is the electron donating ability of the ligands and the difference conferred by pyridyl versus quinolyl donors. Especially within the series of complexes **2**–**4**, which have very similar coordination geometries, this argument appears to be reasonable. Quinoline is a less basic group than pyridine, i.e., a weaker sigma donor to copper ion than pyridine ($pK_b = 8.74$ for pyridine, $pK_b = 9.12$ for quinoline). Thus, less electron density is provided to a copper center when a pyridyl donor is replaced by a quinolyl group, making the Cu-(II)/Cu(I) redox couple more positive, i.e., providing for a more thermodynamically stable Cu(I) species. This same results and trend in redox potentials is observed for isolated copper(I) complexes [LCu]$^+$ with the same series of ligands (Table 5).[2] Note that the range in potentials (~0.4–0.45 V) observed over the series [LCu^{II}–Cl]$^+$ (**1**–**4**) and [LCu^I]$^+$ is about the same, while the individual variations between complexes in the series TMPA-TMQA are comparable (Table 5). However, [LCu^{II}-Cl]$^+$ (**1**–**4**) complexes exhibit systematically more negative $E_{1/2}$ values than [LCu]$^+$ species, undoubtedly caused by the presence of the "hard" anionic chloride ligand which would favor ligation to Cu(II) compared to Cu(I).

Hydrophobicity in the Cu complex environment may also play a role in affecting variations in the redox potentials of complexes **1**–**4**. With increased quinolyl for pyridyl substitution in these complexes, the metal-complex local dielectric will decrease with the increase in hydrocarbon non-polar environment. This favors decreased charge and thus the lower oxidation state of a metal complex; the observed trend of increasing redox potentials going through the series **1** → **4** (Table 5) (as well as for LCu^I]$^+$ species)[2] is consistent with such expectations. Similar effects of placing nearby alkyl or aryl substituents on ligand donors for copper complexes have been observed,[44] including in mononuclear[3] and dinuclear[45] copper complexes with pyrazolyl

(39) Solomon, E. I.; Penfield, K. W.; Wilcox, D. E. *Struct. Bonding (Berlin)* **1983**, *53*, 1−57.

(40) Kokoszka, G.; Karlin, K. D.; Padula, F.; Baranowiski, J.; Goldstein, C. *Inorg. Chem.* **1984**, 4378−4380.

(41) Miyoshi, K.; Tanaka, H.; Kimura, E.; Tsuboyama, S.; Murata, S.; Shimizu, H.; Ishizu, K. *Inorg. Chim. Acta* **1983**, *78*, 23−30.

(42) Karlin, K. D.; Sherman, S. E. *Inorg. Chim. Acta* **1982**, *65*, L39−L40.

(43) Augustin, M. A.; Yandell, J. K.; Addison, A. W.; Karlin, K. D. *Inorg. Chim. Acta* **1981**, *55*, L35.

(44) Patterson, G. S.; Holm, R. H. *Bioinorg. Chem.* **1975**, *4*, 257−275.

(45) Sorrell, T. N.; Garrity, M. L.; Ellis, D. J. *Inorg. Chim. Acta* **1989**, *166*, 71−77.

ligand chelates which have been modified by *tert*-butyl substituents, tridentate Cu(I)-ligand complexes with two 6−Me-pyridyl compared to two pyridyl donors,[46] Cu(I) complexes with sterically hindered tris(3-*tert*-butyl- and 3,5-diphenylpyrazolyl)-hydroborate ligands,[47] and in 6-phenylpyridyl substituted TMPA-Cu(I) complexes.[48]

Some further comment is in order concerning redox potentials and the affects of coordination geometry; by definition, the redox potential for a ligand-complex is due to the difference in complex stability (i.e., $K_{formation}$) of copper(I) versus the copper-(II) ligated forms. While we have determined detailed X-ray structures for most of the [LCuII−Cl]+ complexes 1−4, and even [LCuI]+ species (pseudotetrahedral or trigonal pyramidal),[2] there is too much variation to predict redox potentials. In one perhaps relevant case, stability constants (i.e., $K_{formation}$ in water) for similar Cu(I) and Cu(II) complexes of tripodal N2S2 tetradentate ligands were determined. Here it was found that the noticeable difference in observed redox potential (∼0.2 V) could be largely ascribed to differences in (PEAS)Cu(II) vs (PMAS)Cu(II) complex stabilities, with the latter species possessing a five-membered ring chelate which is more thermodynamically stable,[22] copper(I) is quite 'plastic' and chelate ring size differences in PEAS and PMAS did not greatly affect the [(PEAS)Cu(I) vs (PMAS)Cu(I) stability.

PMAS   PEAS
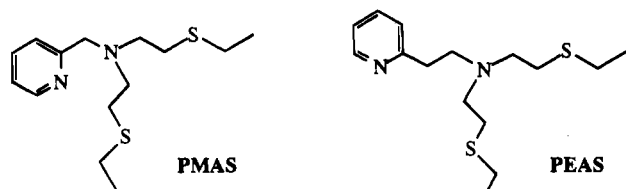
Summary/Conclusions

The pyridyl and/or quinolyl containing tripodal tetradentate ligands readily form pentacoordinate chloro-copper(II) complexes [LCuII−Cl]+, a series of complexes for which the structure and physical properties vary systematically as more quinolyl donors are substituted for pyridyl in the series going from TMPA to TMQA (Chart 1). Like many other [(TMPA)-Cu−X]$^{n+}$ complexes (X =, F−, CH3CN, O2$^{2−}$), [(TMPA)Cu−Cl]+ (1) has a trigonal bipyramidal geometry both in the solid state and in solution, also possessesing the expected UV−vis and EPR spectral characteristics. This geometry is not always observed; in the TMPA-Cu(II) moiety in both of the dinuclear complexes [{(TMPA)Cu}2(μ-CO3$^{2−}$)]$^{2+}$ [49] and [(F8TPP)Fe−O−Cu(TMPA)]+ (F8-TPP = tetrakis(2,6-difluorophenyl)porphyrinate(2−))[50] is distorted very much toward square-based pyramidal, presumably to accomodate the particular steric requirements of the fifth ligand and/or dinuclear structure. As quinolyl donors are synthetically placed into the tripodal tetradentate ligand, both the X-ray structural data and solution physical properties indicate that distortions toward tetragonal (i.e., square-based pyramidal) coordination occur for [LCuII−Cl]+ (L = BPQA, BQPA, TMQA; 2−4). Unfavorable steric interactions of the bulky quinolyl group with the Cl− ion in a trigonal bipyramidal

geometry are seen to be the origin of the distortion; part of the evidence for this conclusion is the observation that [(TMQA)-CuI]+ possesses a trigonal (pyramidal) coordination, where a fith ligand is lacking. An interesting finding is the large range (∼0.45 V) in Cu(II)/Cu(I) redox potential observed for the complexes [LCuII−Cl]+ (1−4), systematically increasing to higher values when L possesses increasing numbers of quinolyl groups.

The deviations in ligand steric effects plus redox potentials translate into substantially varied reactivity of reduced [LCuI]+ complexes with dioxygen.[1,2] Of particular note is that [(BQPA)-Cu]+ reacts with O2 at −80 °C in EtCN to give the 1:1 adduct [(BQPA)Cu(O2)]+, formally a superoxo−copper(II) species. Part of the impetus for the present study was to examine the structures and spectroscopy of these L−Cu(II)−X complexes, with the hope of sheding some light on this or other O2-adducts. The results here indicate that [(BQPA)Cu−X]+ most likely possesses a square-based pyamidal environment, with the anionic X group located in the basal plane. Unfortunately, the presence of strong charge-transfer absorptions in [(BQPA)Cu-(O2)]+, including those due to a small amount of dinuclear [{-(BQPA)Cu}2(O2)]+ which is always present, does not allow us to get a clear picture of the d−d region of the spectrum for the mononuclear complex; [(BQPA)Cu(O2)]+ is also EPR silent.[2] Never-the-less, a "terminal" end-on superoxo ligation seems to be a likely coordination in this complex, where the O2− ligand takes the place of the Cl− ligand in [(BQPA)Cu(Cl)]+ (3). We have noticed that [(BQPA)Cu(O2)]PF6 is more stable at −80 °C in EtCN than [(BQPA)Cu(O2)]ClO4 (hours vs minutes);[2] this seems consistent with the idea that an oxygen-atom in ClO4− can compete for Cu(II) coordination with the weakly end-on bound superoxide anion.

end-on   η², side on
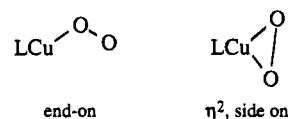
Such a coordination is most often proposed,[51] in a manner known to occur for many M-O2 1:1 adducts such as oxy-hemoglobin or oxy-myoglobin and Schiff-base cobalt(III)-superoxo complexes.[29,52] However, we cannot rule out a η² side-on binding in [(BQPA)Cu(O2)]+,[2] one which would provide strong coordination of the superoxo ligand (i.e., with two Cu−O bonds instead of one),[53] in a pseudooctaheral geometry about the copper ion. This seems less likely on steric grounds, in the presence of the bulky quinolyl ligands in BQPA. Clearly, the suppositions or specualtions described here regarding the structural details of [(BQPA)Cu(O2)]+ can only be confirmed via future direct structural studies on this species. Note, that a superoxo cobalt(III) complex Tp′Co−(O2) (Tp′ = hydrotris(3-*tert*-butyl-5-methylpyrazolyl)borate), possesses a η² side-on binding configuration.[54]

In conclusion, synthetically derived tripodal tetradentate ligands such as those described here offer a wealth of interesting copper(I) and copper(II) chelate chemistry, and changes such as quinolyl for pyridyl donor group offer a way to systematically

(46) Nasir, M. S.; Jacobson, R. R.; Zubieta, J.; Karlin, K. D. *Inorg. Chim. Acta* **1993**, *203*, 5−7.

(47) Carrier, S. M.; Ruggiero, C. E.; Houser, R. P.; Tolman, W. B. *Inorg. Chem.* **1993**, *32*, 4889−4899.

(48) Chuang, C.-L.; Canary, J. W.; Lim, K.; Chen, Q.; Zubieta, J. *Abstracts of Papers*; 208th National Meeting of the American Chemical Society; August 21−25, 1994, Washington, DC, American Chemical Society: Washington, DC, 1994; INOR 352.

(49) Tyeklár, Z.; Paul, P. P.; Jacobson, R. R.; Farooq, A.; Karlin, K. D.; Zubieta, J. *J. Am. Chem. Soc.* **1989**, *111*, 388−389.

(50) Nanthakumar, A.; Fox., S.; Murthy, N. N.; Karlin, K. D.; Ravi, N.; Huynh, B. H.; Orosz, R. D.; Day, E. P.; Hagen, K. S. *J. Am. Chem. Soc.* **1993**, *115*, 8513−8514.

(51) (a) Thompson, J. S. *J. Am. Chem. Soc.* **1984**, *106*, 4057−4059. (b) Thompson, J. S. In *Biological & Inorganic Copper Chemistry*; Karlin, K. D., Zubieta, J., Eds.; Adenine Press: Guilderland, NY, 1986; Vol. 2, pp 1−10.

(52) (a) Niederhoffer, E. C.; Timmons, J. H.; Martell, A. E. *Chem. Rev.* **1984**, *84*, 137−203. (b) *Oxygen Complexes and Oxygen Activation by Transition Metals*; Martell, A. E., Sawyer, D. T., Eds.; Plenum: New York, 1988.

(53) Baldwin, M. J.; Root, D. E.; Pate, J. E.; Fujisawa, K.; Kitajima, N.; Solomon, E. I. *J. Am. Chem. Soc.* **1992**, *114*, 10421−10431.

(54) Egan, J. W., Jr.; Haggerty, B. S.; Rheingold, A. L.; Sendlinger, S. C.; Theopold, K. H. *J. Am. Chem. Soc.* **1990**, *112*, 2445−2446.

vary structure and metal ion redox potential. This tuning of ligand makeup and resulting metal complex will continue to be useful in the design of reagents which may have a predetermined and desired reactivity or utility.

Experimental Section

Material and Methods. Reagents and solvents used were of commercially available reagent quality unless otherwise stated. All copper complexes were synthesized and characterized in the air. Infrared spectra were recorded in Nujol mulls on a Mattson Galaxy 4030 FT-IR spectrometer. Electron Paramagnetic Resonance (EPR) spectra were obtained in frozen solutions at 77 K with 4-mm-o.d. quartz tubes in a Varian E-4 Model spectrometer operating at X-band. The field was calibrated with a powder sample of diphenylpicrylhydrazyl (DPPH; $g = 2.0037$). Solvents used were DMF with concentrations of copper complexes at $\sim 10^{-3}$ M. The signals obtained were integrated roughly by comparing the intensity observed ($I = h_{1/2}(w_{1/2h})^2$) with that of a known concentration of [(TEPA)Cu(Cl)](PF$_6$)[23] in DMF. The room temperature electron absorption spectra were recorded on a Shimadzu UV-160 spectrometer using quartz cuvettes (1 cm). Electrical conductivity measurements were carried out in acetonitrile solvent with a Barnstead Model PM-70CB conductivity bridge and a YSI model 3403 conductivity cell. The cell constant was determined by using a standard aqueous KCl solution. Room temperature magnetic moments were determined by using a Johnson Matthey magnetic susceptibility balance, which was calibrated by using Hg[Co(SCN)$_4$]. Diamagnetic corrections were calculated from tabulated values of Pascal's Constant.[55]

Synthesis of Cu(II) Complexes: [(BPQA)CuCl]PF$_6$·$^1/_2$CH$_2$Cl$_2$ (2-PF$_6$). To a stirred solution of CuCl$_2$·2H$_2$O (0.171 g, 1 mmol) in 50 mL of CH$_3$OH was added BPQA ligand (0.34 g, 1 mmol). The resulting dark blue solution was allowed to stir for one-half hour whereupon NaPF$_6$ (0.84 g, 5 mmol) in 10 mL of CH$_3$OH was added, causing immediate formation of a dark blue precipitate, with some white residual. The reaction mixture was stirred for 15 min and stored in a freezer overnight. The precipitate was collected and recrystallized twice from CH$_2$Cl$_2$/Et$_2$O, and after air-drying, 0.46 g of dark blue microcrystalline material (79%) was obtained. Anal. Calcd for CuC$_{22.5}$H$_{21}$N$_4$Cl$_2$PF$_6$: C, 43.11, H, 3.38, N, 8.94. Found: C, 43.32, H, 3.42, N, 8.73. IR (Nujol, cm^{-1}), 1609 (s, C=C), 1572 (m, C=C), 843 (vs, PF$_6^-$). UV–vis (CH$_3$CN): λ_{max} nm (ϵ, M^{-1}cm^{-1}) 300 (5800), 316 (4650), 700 (sh, 106), 897 (150). Molar conductivity (CH$_3$CN): 145 Ω^{-1}cm^{2}mol^{-1}. EPR (DMF): $g_{\parallel} = 2.23$, $A_{\parallel} = 119 \times 10^{-4}$ cm^{-1}. Magnetic moment (solid state, room temperature): $\mu_{eff} = 1.87$ μ_B/Cu. X-ray quality crystals of this compound [(BPQA)CuCl]PF$_6$·1/2Et$_2$O were obtained by recrystallizing the copper(II) complex from acetonitrile/ether.

[(BQPA)CuCl]PF$_6$ (3-PF$_6$). BQPA (0.200 g, 0.51 mmol) and CuCl$_2$·2H$_2$O (0.092 g, 0.51 mmol) were mixed in 10 mL of CH$_3$OH solvent, giving a blue solution. After stirring one-half-hour, NaPF$_6$ (0.45 g, 2.7 mmol) in 10 mL of CH$_3$OH was added, causing an immediate change to light green. After one-half hour of stirring, a light green solid formed. This was collected and recrystallized three times from CH$_2$Cl$_2$/Et$_2$O, and dried *in vacuo*, giving 0.258 g of light green microcrystalline material (75%). Anal. Calcd for CuC$_{26}$H$_{22}$N$_4$ClPF$_6$: C, 49.22, H, 3.50; N, 8.83. Found: C, 49.49 H, 3.61 N, 8.77 IR (Nujol, cm^{-1}), 1601 (s, C=C), 1570 (m, C=C), 847 (vs, PF$_6^-$). UV–vis (CH$_3$CN): λ_{max} nm (ϵ, M^{-1}cm^{-1}) 300 (15000), 316 (12400), 737 (sh, 137), 862 (139). Molar conductivity (CH$_3$CN): 140 Ω^{-1}cm^{2}mol^{-1}. EPR (DMF): $g_{\parallel} = 2.27$, $A_{\parallel} = 127 \times 10^{-4}$ cm^{-1}. Magnetic moment (solid state, room temperature): $\mu_{eff} = 1.92$ μ_B/Cu.

[(TMQA)CuCl]PF$_6$ (4-PF$_6$). TMQA ligand (0.3 g, 0.68 mmol) and CuCl$_2$·2H$_2$O (0.116 g, 0.68 mmol) were mixed in 45 mL of CH$_3$OH giving a greenish blue solution. This was allowed to stir at room temperature for one hour and NaPF$_6$ (0.57 g, 3.4 mmol) in 10 mL of CH$_3$OH solvent was added, whereupon the solution immediately changed to light blue; some white residual also gradually formed. After

stirring for 30 min, the solid was collected by filtration using a medium frit. This was recrystallized twice from CH$_2$Cl$_2$/Et$_2$O, and dried *in vacuo*, giving 0.21 g of a blue microcrystalline material (50% yield). Anal. Calcd for CuC$_{30}$H$_{24}$N$_4$ClPF$_6$: C, 52.64, H, 3.53; N, 8.18. Found: C, 52.16 H, 3.59 N, 8.17. IR (Nujol, cm^{-1}), 1620 (s, C=C), 1603 (vs, C=C), 1572 (m, C=C), 840 (vs PF$_6^-$). UV–vis (CH$_3$CN): λ_{max} nm (ϵ, M^{-1}cm^{-1}) 303 (20200), 316 (15800), 691 (185), 1000 (90). Molar conductivity (CH$_3$CN): 140 Ω^{-1}cm^{2}mol^{-1}. EPR (DMF): $g_{\parallel} = 2.26$, $A_{\parallel} = 137 \times 10^{-4}$ cm^{-1}. Magnetic moment (solid state, room temperature): $\mu_{eff} = 1.97$ μ_B/Cu. X-ray quality crystals of this compound [(TMQA)CuCl]PF$_6$·CH$_3$CN·0.5Et$_2$O were obtained by recrystallizing the copper(II) complex from acetonitrile/ether.

X-ray Structure Determination of [(BPQA)CuCl]PF$_6$·0.5Et$_2$O and [(TMQA)CuCl]PF$_6$·CH$_3$CN·0.5Et$_2$O. A blue cubic crystal of 2-PF$_6$·0.5Et$_2$O, $0.25 \times 0.25 \times 0.40$ mm, was mounted on a glass fiber. All measurements were made on a Rigaku AFC6S diffractometer with a graphite monochromated Mo Kα source (λ (MoKα) = 0.71069 Å). Cell constants and an orientation matrix for data collection, obtained from a least-squares refinement using the setting angles of 25 carefully centered reflections in the range $31.20 < 2\theta < 37.88°$ corresponded to a monoclinic cell with dimensions shown in Table 1. All data were collected at -120 °C using the ω scan technique to a maximum 2θ value of 50.0°. Of the 4664 reflections which were collected, 4486 were unique ($R_{int} = 0.050$). The linear absorption coefficient for MoKα is 11.3 cm^{-1}. Azimuthal scans of several reflections indicated no need for an absorption correction. Crystal and data collection details are provided in Table 1. The compound has a half ether molecule as a solvent of crystallization, which is disordered. Its coordinates were fixed at the final stages of refinement.

A blue crystal of 4-PF$_6$·CH$_3$CN·0.5Et$_2$O, having approximate dimensions of $0.20 \times 0.20 \times 0.25$ mm was mounted on a glass fiber. All measurements were made on a Rigaku AFC6S diffractometer with a graphite monochromated Mo Kα source (λ(MoKα) = 0.710 69 Å). Cell constants and an orientation matrix for data collection, obtained from a least-squares refinement using the setting angles of 25 carefully centered reflections in the range $24.08 < 2\theta < 37.87°$ corresponded to a monoclinic cell with dimensions shown in Table 1. All data were collected at -110 °C using the ω scan technique to a maximum 2θ value of 49.9°. Of the 6057 reflections which were collected, 5938 were unique ($R_{int} = 0.059$). The linear absorption coefficient for Mo Kα is 8.8 cm^{-1}. Azimuthal scans of several reflections indicated no need for an absorption correction. Crystal and data collection details are provided in Table 1. Due to the disordered solvent molecules of crystallization, the coordinates of the CH$_3$CN and half of ether were fixed at the final stages of refinement. All data processing was performed on a VAX 3520 workstation using the TEXSAN (Moleclular Structure Corp.) crystallographic package.

Electrochemistry. Cyclic voltammetry and bulk electrolysis were carried out by using a Bioanalytical Systems BAS-100B Electrochemistry Analyzer connected with a HP-7440A plotter. The cell consisted of a modification of a standard three chambered design equipped for handling of air sensitive solutions by utilizing high vacuum valve (Viton O-ring) seals. Either a platinum disk (BAS MF 2013) or a glassy carbon electrode (GCE, BAS MF 2012) was used as the working electrode. The reference electrode was Ag/AgNO$_3$. The measurements were performed at room temperature in DMF solvent containing 0.2 M tetrabutylammonium hexafluorophosphate (TBAHP) and 10^{-3}–10^{-4} M copper complex deoxygenated by bubbling argon through it.

Supplementary Material Available: List of anisotropic thermal parameters, and intramolecular bond distances and angles for (2-PF$_6$) and (4-PF$_6$) (8 pages). Ordering information is given on any current masthead page.

(55) O'Connor, C. J. *Prog. Inorg. Chem.* **1982**, *29*, 203.